Polycrystalline materials with pores: effective properties through a boundary element homogenization scheme.

F. Trentacoste[1], I. Benedetti[1a] and M.H. Aliabadi[2b]

[1] Dipartimento di Ingegneria Civile, Ambientale, Aerospaziale e dei materiali, Università degli Studi di Palermo, Viale delle Scienze, Edificio 8, 90128, Palermo, Italy

[2] Department of Aeronautics, Imperial College London, South Kensington Campus,SW7 2AZ, London, UK

[a]ivano.benedetti@unipa.it, [b]m.h.aliabadi@imperial.ac.uk

Keywords: Polycrystalline materials, Micromechanics, Porosity, Boundary element method.

Abstract. In this study, the influence of porosity on the elastic effective properties of polycrystalline materials is investigated using a formulation built on a boundary integral representation of the elastic problem for the grains, which are modeled as 3D linearly elastic orthotropic domains with arbitrary spatial orientation. The artificial polycrystalline morphology is represented using 3D Voronoi tessellations. The formulation is expressed in terms of intergranular fields, namely displacements and tractions that play an important role in polycrystalline micromechanics. The continuity of the aggregate is enforced through suitable intergranular conditions. The effective material properties are obtained through material homogenization, computing the volume averages of micro-strains and stresses and taking the ensemble average over a certain number of microstructural samples. In the proposed formulation, the volume fraction of pores, their size and distribution can be varied to better simulate the response of real porous materials. The obtained results show the capability of the model to assess the macroscopic effects of porosity.

Introduction

Polycrystalline materials, such as metals, ceramics and alloys, are widely used in many applications of engineering interest. The internal structure of a polycrystalline material is determined by the size and shape of the grains, by their crystallographic orientation and by different type of defects within them. For this reason the investigation of the link between their micro and macro-properties has attracted considerable attention [1].

Depending on the manufacturing conditions, several polycrystalline materials present, at the microscale, a regular arrangement of their grains: their microstructure is characterized by grains with uniform size and identical morphology. This holds in particular for several polycrystalline films. Examples of materials with regular microstructure are *In-N* and MgF_2 films, Yttria and Alumina.

In this paper, a computational model for the homogenization of polycrystalline materials with regular microstructure (grain size distribution and morphology) *and pores* is developed. Even if the study is referred to polycrystals with regular microstructure, the formulation is able to take into account polycrystals with a random size distribution and morphology of their grains. The results were compared with the trend predicted by the Spriggs equation, which is widely used to fit experimental measurements when porous material are considered.

Generation of artificial regular microstructure

The microstructure of polycrystalline materials can be reconstructed experimentally or it can be artifcially generated using algorithms able to retain the main statistical topological, morphological and crystallographic features of the polycrystalline aggregates. Although the experimental characterization may provide fundamental information, it generally requires expensive equipment and complicated and time consuming post-processing. The use of suitable computer models offers the opportunity of simulating large numbers of microstructures, complementing and reducing the experimental effort.

In the case of polycrystalline materials, the Voronoi tessellation is widely recognized and used for the generation of the microstructural model [2]. The Voronoi cells are convex polyhedra bounded by at polygonal faces, which makes them particularly suitable for numerical treatment. For such reasons, three-dimensional Voronoi tessellations are used in the present study to generate microstructures with regular grain

distribution, size and orientation. The topology and morphology of the tessellation is controlled by the arrangement of the initial seeds. On the basis of this consideration, it is possible to generate different regular morphologies. In particular, common regular morphologies can be obtained by using regularly spaced seeds distributions: a cubic array of seeds provides cubes, collocating the seeds on the sites of a face-centered cubic structure provides runcated octahedra, while the body-centered structure provides dodecahedra. Considering the microstructural morphologies, it is possible to distinguish among:

- Cubic structure;

- Hexarhombic dodecahedron structure;

- Rhombic dodecahedron structure;

- Truncated octahedra structure.

In Fig.(1) samples of the different types of regular microstructure are shown.

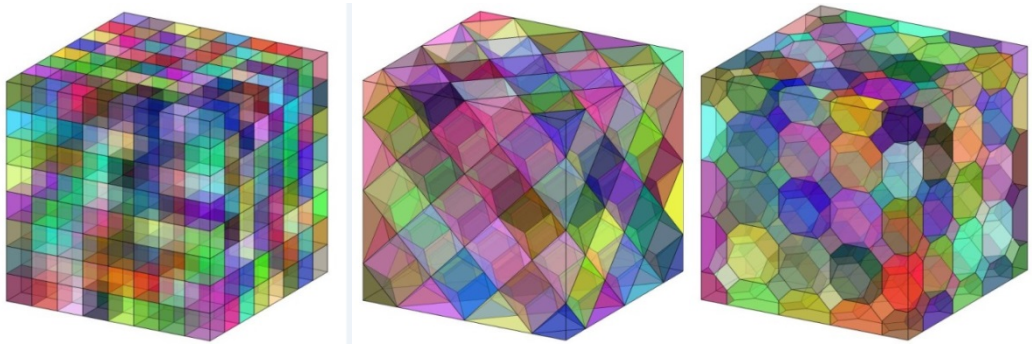

Fig.1: Samples of the different types of regular microstructures.

Three-dimensional Grain boundary element formulation

In the present work the numerical model for the single crystal is obtained by using the Boundary Element Method (BEM) for three-dimensional anisotropic elasticity. The polycrystalline aggregate is modeled as a multi-region boundary element problem, so that different elastic properties and crystallographic orientation can be assigned to each grain. Each grain is represented as a Voronoi cell G_k bounded by the surface B^k, which is formed by the union of at convex polygonal faces F_j^k. On the surfaces of the domain boundary grains generated by the intersection with the external boundary B of the analysis region some quantities, either displacements or tractions, are prescribed as external boundary conditions (BCs) that is [3]:

$$u_i^k = \bar{u}_i^k \quad or \quad t_i^k = \bar{t}_i^k \quad i = 1, \dots, 3 \quad on\ G_k \tag{1}$$

where u_i^k e t_i^k are components of displacement and tractions on B^k and the overbar denotes prescribed quantities. The remaining unknown quantities are determined by the solution of the numerical model. On the other hand, both displacements and tractions are unknown at the interfaces between two adjacent grains G_a and G_b. For this reason, displacement continuity and traction equilibrium equations must be enforced:

$$\tilde{u}_i^a - \tilde{u}_i^b = 0 \qquad \tilde{t}_i^a - \tilde{t}_i^b = 0 \tag{2}$$

where the tilde indicates quantities expressed in the local grain face reference system: opposite reference systems are associated to the two faces, of two different grains, meeting at a given interface. Considering a given grain, with its own crystallographic orientation, *the displacement boundary integral equation* can be written, in the face local reference system, as [4]:

$$\tilde{c}_{ij}^k(\boldsymbol{y})\tilde{u}_j^k(\boldsymbol{y}) + \sum_{q=1}^{N_f^k} \int_{F_q^k} \tilde{T}_{ij}^k(\boldsymbol{x},\boldsymbol{y})\, \tilde{u}_j^k(\boldsymbol{x})\, dF(\boldsymbol{x}) = \sum_{q=1}^{N_f^k} \int_{F_q^k} \tilde{U}_{ij}^k(\boldsymbol{x},\boldsymbol{y})\, \widetilde{ut}_j^k(\boldsymbol{x})\, dF(\boldsymbol{x}) \tag{3}$$

where the $\tilde{U}_{ij}^k$ and $\tilde{T}_{ij}^k$ are the displacement and the traction fundamental solution, see Benedetti and Aliabadi for further details [3]. To solve the polycrystalline problem eq (3) written for each grain $G_k, k\ 1; \dots;\ N_g$, is discretized following the classical BEM discretization procedure, which leads to the equation for each grain:

$$[\,\tilde{\mathbf{H}}^{\mathbf{k}}_{\mathbf{nc}} \quad \tilde{\mathbf{H}}^{\mathbf{k}}_{\mathbf{c}}]\begin{bmatrix}\tilde{\mathbf{u}}^{\mathbf{k}}_{\mathbf{nc}}\\ \tilde{\mathbf{u}}^{\mathbf{k}}_{\mathbf{c}}\end{bmatrix} = [\tilde{\mathbf{G}}^{\mathbf{k}}_{\mathbf{nc}} \quad \mathbf{G}^{\mathbf{k}}_{\mathbf{c}}]\begin{bmatrix}\tilde{\mathbf{t}}^{\mathbf{k}}_{\mathbf{nc}}\\ \tilde{\mathbf{t}}^{\mathbf{k}}_{\mathbf{c}}\end{bmatrix} \tag{4}$$

The system of equations for the entire polycrystalline aggregate is obtained by writing the previous set of equation for each grain and enforcing the boundary and interface conditions on the overall aggregate. The final system of equation is written:

$$\begin{bmatrix} \boldsymbol{A^1} & \boldsymbol{B^1} & \mathbf{0} & & \cdots & \mathbf{0} \\ \mathbf{0} & \boldsymbol{A^2} & \boldsymbol{B^2} & & \cdots & \mathbf{0} \\ \vdots & & & \ddots & & \\ \mathbf{0} & & \ldots & \mathbf{0} & \boldsymbol{A^{N_g}} & \boldsymbol{B^{N_g}} \\ & & & \mathbf{IC_u} & & \\ & & & \mathbf{IC_t} & & \end{bmatrix}\begin{bmatrix}\mathbf{x}^{\mathbf{1}}_{\mathbf{nc}}\\ \mathbf{x}^{\mathbf{1}}_{\mathbf{c}}\\ \vdots\\ \mathbf{x}^{\mathbf{N_g}}_{\mathbf{nc}}\\ \mathbf{x}^{\mathbf{N_g}}_{\mathbf{c}}\end{bmatrix} = \begin{bmatrix}\mathbf{C}^{\mathbf{1}}\,\mathbf{x}^{\mathbf{1}}_{\mathbf{nc}}\\ \mathbf{C}^{\mathbf{2}}\,\mathbf{x}^{\mathbf{1}}_{\mathbf{c}}\\ \vdots\\ \mathbf{C}^{\boldsymbol{N_g}}\mathbf{y}^{\boldsymbol{N_g}}_{\mathbf{nc}}\\ \mathbf{0}\\ \mathbf{0}\end{bmatrix} \tag{6}$$

where the matrix blocks $\boldsymbol{A^k}$ contains columns from the matrices $\tilde{\mathbf{H}}^{\mathbf{k}}_{\mathbf{nc}}$ and $-\tilde{\mathbf{G}}^{\mathbf{k}}_{\mathbf{nc}}$ corresponding to the unknown components of $\tilde{\mathbf{u}}^{\mathbf{k}}_{\mathbf{nc}}$ and $\tilde{\mathbf{t}}^{\mathbf{k}}_{\mathbf{nc}}$ that are collected in $\tilde{\mathbf{x}}^{\mathbf{k}}_{\mathbf{nc}}$, the blocks $\boldsymbol{C^k}$ collect columns from $-\tilde{\mathbf{H}}^{\mathbf{k}}_{\mathbf{nc}}$ and $\tilde{\mathbf{G}}^{\mathbf{k}}_{\mathbf{nc}}$ corresponding to the known components of $\tilde{\mathbf{u}}^{\mathbf{k}}_{\mathbf{nc}}$ and $\tilde{\mathbf{t}}^{\mathbf{k}}_{\mathbf{nc}}$, i.e. the BCs, that are collected in $\mathbf{y}^{\mathbf{k}}_{\mathbf{nc}}$, $\boldsymbol{B^k} = |\,\tilde{\mathbf{H}}^{\mathbf{k}}_{\mathbf{nc}} \; -\tilde{\mathbf{G}}^{\mathbf{k}}_{\mathbf{nc}}\,|$, the vectors $\mathbf{x}^{\mathbf{k}}_{\mathbf{c}}$collect the unknown interface displacements and tractions of the k-th grain and the matrices $\mathbf{IC_u}$ and $\mathbf{IC_t}$, whose lines contain only 1 and -1 and zeros, implement respectively the displacement and traction interface conditions in the system matrix. System (6) is highly sparse and the use of specialized sparse solvers is then desirable to speed up its solution. In this work PARDISO has been used as a solver. Details about the discretization process are given in Benedetti and Aliabadi [3].

Computational material homogenization

An important goal of the mechanics and physics of heterogeneous materials is the derivation of their properties from the constitutive laws and spatial distribution of their micro-components. This estimation is referred to as material homogenization and it is the main task of micromechanics [5]. The material homogenization is usually performed by evaluating volume and ensemble averages of some relevant fields over one or more realizations of the microstructure subjected to suitable boundary conditions, and then linking these averaged fields by means of effective properties [6,7].

Given a polycrystalline realization $R(N_g)$, consisting of N_g grains subjected to consistent boundary conditions, since the material is supposed to not develop microcracks, stress and strain volume averages can be used to extract the apparent elastic moduli. Stress and strain volume averages are defined by:

$$\Gamma_{ij} = \frac{1}{V}\int_V \gamma_{ij}(x)dV(x) = \frac{1}{2V}\int_{\partial V}(u_i\, n_j + u_i n_j)dS \tag{7}$$

$$\Sigma_{ij} = \frac{1}{V}\int_V \sigma_{ij}(x)dV(x) = \frac{1}{V}\int_{\partial V}(x_i\, t_j)dS \tag{8}$$

where the integrals over the microstructure volume V are transformed into surface integrals over the volume boundary ∂V, as consequence of the divergence theorem. Lower case letters in Eq.(7,8) refer to micro-scale quantities, i.e. displacements, tractions, strains and stresses in the polycrystalline microstructure, while capital Greek letters refer to homogenized quantities. Once the stress $\boldsymbol{\Sigma}$ and strain $\boldsymbol{\Gamma}$ macro-fields are known, the apparent macro-properties are defined by:

$$\boldsymbol{\Sigma} = \widehat{\boldsymbol{C}}\,\boldsymbol{\Gamma} \tag{9}$$

where the hat denotes *apparent overall properties*, to distinguish them from the microscopic ones. This relationship is the homogenized stress-strain equation and forms the basis for the homogenization procedure. The apparent properties, eq.(9), are computed for each considered microstructural realization and an ensemble average is eventually performed over the number of realizations.

In the present work, the effective properties of polycrystalline yttria are first analyzed. Single crystals of Yttria present cubic morphology at the grain scale and cubic material symmetry [8]. It is characterized by three elastic constants C_{11}, $C_{12}$and C_{44} being $C_{14} = C_{15} = C_{16} = 0$, $C_{24} = C_{25} = C_{26} = 0$, $C_{34} = C_{35} = C_{136} = 0$; the stiffness matrix in the material reference system can be written in Voigt notation as:

$$\mathbf{C} = \begin{bmatrix} C_{11} & C_{11} & C_{11} & 0 & 0 & 0 \\ C_{11} & C_{11} & C_{11} & 0 & 0 & 0 \\ C_{11} & C_{11} & C_{11} & 0 & 0 & 0 \\ 0 & 0 & 0 & C_{11} & 0 & 0 \\ 0 & 0 & 0 & 0 & C_{11} & 0 \\ 0 & 0 & 0 & 0 & 0 & C_{11} \end{bmatrix} \tag{10}$$

To assess the capability and accuracy of the formulation, it is interesting to compute all the entries of the effective stiffness matrix, Eq.(10). For this purpose, it is necessary to perform six different computations, corresponding to the six linearly independent load cases for the unit cell. N_t = 10 aggregates with N_g = 125 grains and subjected to kinematic uniform boundary conditions have been simulated. The apparent obtained stiffness matrix is:

$$\hat{\mathbb{C}} = \begin{bmatrix} 233.1 & 103.7 & 103.6 & 1.036 & -0.02 & -0.104 \\ 103.7 & 233.1 & 103.6 & -0.138 & 0.92 & 0.018 \\ 103.6 & 103.6 & 233.2 & -0.027 & -0.06 & 0.938 \\ 0.02 & 0.628 & -0.23 & 64.92 & 0.73 & 0.027 \\ 0.74 & -0.06 & -0.25 & 0.71 & 65 & 0.133 \\ 0.66 & -0.2 & 0.01 & 0.56 & 0.12 & 65.03 \end{bmatrix} \tag{11}$$

It is interesting to observe that the isotropy of the microstructural aggregate is confirmed by the structure of the effective stiffness matrix. Given an unit cell with N_g crystals, in general also for a isotropic material, the assumption of overall isotropic behavior of the unit cell may be restrictive and should be verified. However, if a suitable number of realizations/grains is considered the effective stiffness matrix assumes soon an isotropic structure. The values of the effective elastic moduli E and G for polycrystalline Y_2O_3 have been reported by various authors. In this study, the overall values, are $E = 175$ GPa and $G = 65$ GPa, which are in very good agreement with the values $E = 174$ GPa and $G = 66.5$ GPa, reported by Palko at al.[8]. The aggregate properties of alumina are also computationally investigated. Alumina Al_2O_3 mono-crystals are characterized by the following stiffness matrix:

$$\mathbb{C} = \begin{bmatrix} \mathrm{C}_{11} & \mathrm{C}_{12} & \mathrm{C}_{13} & \mathrm{C}_{14} & 0 & 0 \\ \mathrm{C}_{21} & \mathrm{C}_{22} & \mathrm{C}_{23} & \mathrm{C}_{24} & 0 & 0 \\ \mathrm{C}_{31} & \mathrm{C}_{32} & \mathrm{C}_{33} & 0 & 0 & 0 \\ \mathrm{C}_{41} & \mathrm{C}_{42} & 0 & \mathrm{C}_{44} & 0 & 0 \\ 0 & 0 & 0 & 0 & \mathrm{C}_{55} & \mathrm{C}_{56} \\ 0 & 0 & 0 & 0 & \mathrm{C}_{65} & \mathrm{C}_{66} \end{bmatrix} \tag{12}$$

being $C_{11} = C_{22}$; $C_{13} = C_{23}$; $C_{44} = C_{55}$; $C_{14} = -C_{24} = C_{56}$; $C_{66} = 1/2(C_{11} - C_{22})$. The homogenization procedure leads, for the alumina polycrystalline to the following effective stiffness matrix:

$$\tilde{\mathbb{C}} = \begin{bmatrix} 473.1 & 143.3 & 143.4 & 1.179 & -0.101 & -0.641 \\ 143.3 & 472.4 & 143.7 & 0.209 & 1.348 & 0.302 \\ 143.4 & 143.7 & 472.8 & -0.458 & -0.624 & 1.214 \\ -0.1 & 1.942 & -0.863 & 165.2 & 1.68 & 0.424 \\ 1.67 & 0.01 & -1.05 & 1.692 & 164.6 & 0.072 \\ 1.2 & -0.26 & -0.002 & 1.48 & 0.03 & 164.7 \end{bmatrix} \tag{13}$$

Again, macroscopic isotropy is observed. The values of the effective elastic moduli E and G for polycrystalline Al_2O_3 have been reported by various authors [8]. In this study, the average values, calculated over $N_r = 10$ realizations of aggregates with N_g =189 grains, are $E = 405{,}5$ GPa and $G = 165$ GPa, which are in very good agreement with the values $E = 402{,}7$ GPa and $E = 163{,}4$ GPa, reported by Pabst et al. who extrapolated the values to zero porosity.

Polycrystalline materials with pores: the Spriggs law for the estimation of the effective properties

Material porosity is related to the lack of solidification due to the fact that there are not enough atoms present to fill the available space. This is different from the case of void inclusion, related to the presence of gas atoms during the nucleation process.

The effects of porosity on the elastic properties of polycrystalline materials have been studied by various investigators and a number of expressions have been proposed. H. Spriggs suggested an exponential equation

able to fit a wide set of data for aluminum oxide over a wide range of porosity [10]. According to his equation, the Young and shear moduli of a porous polycrystalline material can be expressed as:

$$E(P) = E_0\, e^{-b_E P} \qquad G(P) = G_0\, e^{-b_G P} \tag{14}$$

where $E(P)$ and $G(P)$are the values of the elastic moduli at the current value of porosity P, expressed as pores volume fraction, and E_0 and G_0 are the values for the zero porosity case. Eqs.(14) have been widely used to predict the elastic moduli of porous brittle solids. The empirical constants b_E and b_G, associated with a given manufacturing technique, are related to the proportions of closed and open pores within the polycrystalline aggregates.

In the aforementioned grain boundary formulation, to take into account the presence of pores, in the proposed formulation the following steps are followed:

(i) The missing grains (pores) are localized and given a specific flag within the generated tessellation;

(ii) The computation of the BE matrices H and G is skipped for the aged grains and they are not considered in the population of the final system, leading to a consequent reduction of its order;

(iii) Free traction boundary conditions are enforced, instead of interface continuity and equilibrium equations, on the faces of the grains adjacent to the missing ones (pores).

From the numerical point of view, when pores are considered, the number of rows and columns of the final system is reduced according to

$$\mathrm{SO} = N_0 - 6\,N_i - 3N_e \tag{15}$$

where N_0 is the system order when no grains have been removed and N_i and N_e are the number of interface and external boundary nodes related to the missing grains.

To simulate porosity for yttria, $N_r = 50$ microstructures of N_g =512 cubic grains have been considered. In each of then a different distribution of pores has been chosen to better simulate the response of a real porous material. Then, the computed effective properties have been compared with the values predicted by the Spriggs law, over a given range of porosity (Fig.2), showing the capability of the model to assess the macroscopic effect of pores.

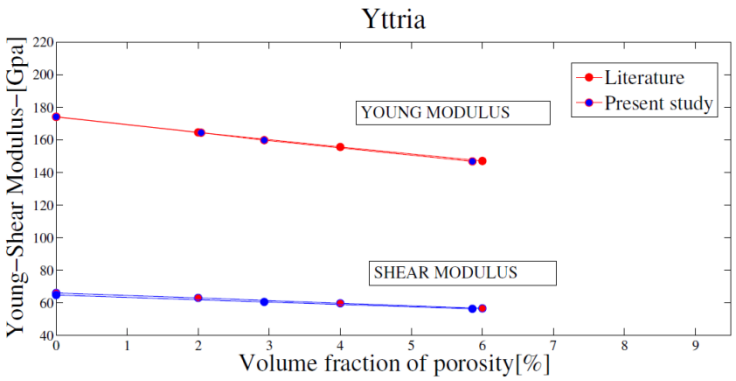

Fig.2: Young and shear moduli of $Y_2\,O_3$ as function of volume fraction of porosity.

For alumina $N_r = 50$ microstructures with N_g =189 truncated octahedral grains have been considered. As it possible to see in (Fig. 3), also in this case what is obtained is in very good agreement with the trend predicted by the Spriggs equation.

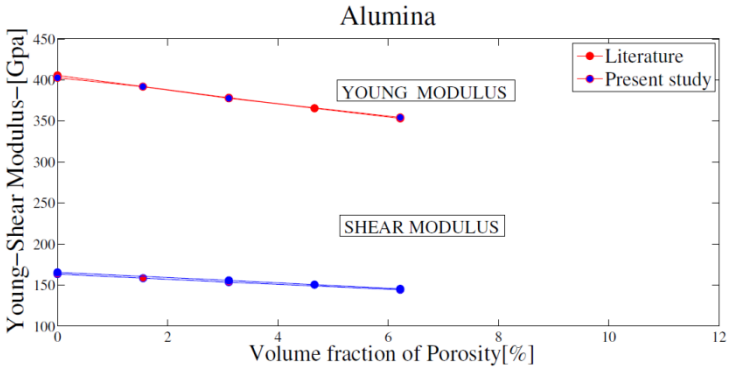

Fig.3: Young and shear moduli of $Al_2\ O_3$as function of volume fraction of porosity.

Conclusions

In the present work, a three dimensional grain boundary formulation has been proposed for studying the effect of porosity on the elastic properties of polycrystalline materials. The formulation is based on the boundary integral representation of the three-dimensional anisotropic elastic problem for the crystals of the aggregate. The method has been applied to the determination of the effective properties of some polycrystals with a regular microstructural morphologies and the results are in good agreement with literature data in the framework of numerical homogenization. The results obtained in case of porosity have been successfully compared with the Spriggs equation for the analyzed polycrystalline materials. Further studies may consider the microstructural damage evolution when the presence of pores is considered.

References

[1] B. Adams, T. Olson, Progress in Materials Science 43, 188 (1998).
[2] C. Rycroft, Chaos 19,(2009) 041111.
[3] I. Benedetti, M.H. Aliabadi, Computational Material Science 67, 249260 (2013).
[4] M. Aliabadi, The Boundary Element Method: Application in Solids and Structures Vol.2 (John Wiley and Sons Ltd., England, 2002).
[5] S. Nemat-Nasser, M. Hori, Micromechanics: Overall Properties of Heterogeneous Materials, Second Revised Edition. (North-Holland, Elsevier, Amsterdam, The Netherlands,1999).
[6] M. Ostoja-Starzewski, Probabilistic Engineering Mechanics 21, 112132 (2006).
[7] T. Kanit, S. Forest, I. Galliet, V. Mounoury, D. Jeulin, International Journal of Solids and Structures 40, 36473679, (2003).
[8] J.W. Palko, W.M. Kriven, S. V. Sinogeikin, J.D. Bass and A. Sayir Journal of appliedphysics 89, 7792-7796, (2001).
[9] W. Pabst, G. Tichà, E. Gregorovà, Ceramics 48, 41-48, (1961).
[10] R.M. Spriggs, Journal of the American Ceramic Society 44, 628-629, (1961).